



Determination of optimum isotherm and kinetic models for phosphate sorption onto iron oxide nanoparticles: nonlinear regression with various error functions

Jeong-Ann Park^a, Jae-Hyun Kim^a, Jin-Kyu Kang^a, Jeong-Woo Son^a, In-Geol Yi^a,
Song-Bae Kim^{a,b,*}, Sang-Hyup Lee^{c,d}, Jae-Woo Choi^c, Chang-Gu Lee^c

^aEnvironmental Functional Materials & Biocolloids Laboratory, Seoul National University, Seoul 151-921, Korea, Tel. +82 2 880 4587; email: songbkim@snu.ac.kr (S.-B. Kim)

^bDepartment of Rural Systems Engineering and Research Institute of Agriculture and Life Sciences, Seoul National University, Seoul 151-921, Korea

^cCenter for Water Resource Cycle Research, Korea Institute of Science and Technology, Seoul 136-791, Korea

^dGraduate School of Convergence Green Technology & Policy, Korea University, Seoul 136-701, Republic of Korea

Received 24 February 2014; Accepted 28 October 2014

ABSTRACT

The aim of this study was to determine optimum kinetic and isotherm models for phosphate (P) sorption onto iron oxide nanoparticles through nonlinear regression analysis. Equilibrium batch experiments were conducted at the experimental conditions of initial P concentration = 0.5–20 mg/L, adsorbent doses = 0.1, 0.2, 0.3, 0.4, 0.5, and 0.6 g/L, and shaking time = 24 h. Kinetic batch experiments were also performed at the experimental conditions of initial P concentrations = 1, 2, 4, 6, 8, and 10 mg/L, adsorbent dose = 0.6 g/L, and shaking time = 10 min–24 h. Six isotherm models (Langmuir, Freundlich, Temkin, Redlich–Peterson, Khan, and Sips) were used to analyze the equilibrium data through nonlinear regression analysis. Three kinetic models (pseudo-first-order, pseudo-second-order, and Elovich) were used to analyze the kinetic data through nonlinear regression. Error functions including the sum of the squared errors, hybrid fractional error function (HYBRID), average relative error, Marquardt's percent standard deviation, and sum of the absolute errors (EABS) were used to minimize the error distribution between experimental data and predicted model fits in the optimization process. To compare the five error values, the results of each set were normalized and summed. Considering both coefficient of determination (R^2) and Chi-square (χ^2), the Redlich–Peterson (Freundlich) model was found to provide the best fit to the experimental data in the equilibrium model analyses, and the optimum parameter values were obtained by the HYBRID error function with the parameter values of $K_R/a_R = 3.59$ – 4.15 mg/g and $g = 0.69$ – 0.89 from the Redlich–Peterson model. Considering both R^2 and χ^2 , the Elovich (or pseudo-second-order) model was found to provide the best fit to the kinetic data in the kinetic model analyses, and the optimum parameter values produced by the EABS error function with the parameter values of $\alpha = (3.60 \times 10^5)$ – (4.80×10^6) mg/g/h and $\beta = 4.43$ – 13.07 g/mg from the Elovich model.

*Corresponding author.

Keywords: Error function; Isotherm model; Iron oxide nanoparticle; Kinetic model; Nonlinear regression; Phosphate sorption

1. Introduction

Adsorption is widely used for the treatment of water and wastewater because of its relatively low cost and simplicity of design and operation [1]. Adsorption characteristics of a contaminant onto an adsorbent are examined via batch sorption tests under various experimental conditions [2]. Equilibrium and kinetic batch tests are used to determine the effectiveness of a specific adsorbent for removing a target adsorbate [3,4]. Equilibrium and/or kinetic sorption models have been used for the analyses of batch sorption data. Zhang et al. [5] investigated the adsorption characteristics of phosphorus onto laterite (red soil) using isotherm models. They performed linear and nonlinear regression analyses to determine the proper adsorption parameters from equilibrium sorption data. Karadag et al. [6] performed a comparative study of linear and nonlinear regressions for ammonium exchange by clinoptilolite using kinetic and isotherm models. Ho et al. [7–12] conducted linear and nonlinear regressions for adsorption of contaminants (e.g. heavy metals and dyes) to adsorbents using kinetic sorption and isotherm models. Kumar et al. [13–18] also performed linear and nonlinear regressions for the adsorption isotherms of basic dyes (e.g. methylene, malachite green, safranin, and basic red 9) on activated carbon. It was reported in the literature [7,19]

that nonlinear regression would be more appropriate for determination of isotherm parameters than linear regression because nonlinear methods avoid problems (alteration of error distribution) that occur during transformation of nonlinear model expression to a linear one. Also, the optimum isotherm parameters for modeling contaminant sorption onto adsorbents vary depending on the error functions used in the optimization process [7].

Phosphate is an essential macronutrient in aquatic environments, but in excessive amounts, it causes eutrophication of water bodies [20]. Recently, iron oxide particles have been used by several researchers for phosphate removal from aqueous solutions [21,22]. de Vicente et al. [23] tested nanosized magnetite (Fe_3O_4) and micron-sized iron (Fe) particles as phosphate adsorbents for lake restoration. They used the Langmuir isotherm model to compare the phosphate adsorption capacity between Fe_3O_4 and Fe particles. Zeng et al. [24] examined adsorptive removal of phosphate using industrial waste iron oxide tailings. They used isotherm and kinetic models to analyze the experimental data.

In this study, optimum kinetic and isotherm models for phosphate sorption onto iron oxide nanoparticles were determined through nonlinear regression analysis by extending the research works of Yoon

Table 1
Nonlinear forms of isotherm and kinetic models used in nonlinear regression analyses

Model	Mathematical expression	Reference
<i>Two-parameter isotherm</i>		
Langmuir	$q_e = \frac{Q_m K_L C_e}{1 + K_L C_e}$ (1)	[26]
Freundlich	$q_e = K_F C_e^{1/n}$ (2)	[27]
Temkin	$q_e = \frac{K_T}{b_T} \ln A_T C_e$ (3)	[28]
<i>Three-parameter isotherm</i>		
Redlich–Peterson	$q_e = \frac{K_R C_e}{1 + a_R C_e^x}$ (4)	[29]
Khan	$q_e = \frac{q_s b_K C_e}{(1 + b_K C_e)^{a_K}}$ (5)	[30]
Sips	$q_e = \frac{q_{mS} C_e^{\beta_s}}{1 + a_S C_e^{\beta_s}}$ (6)	[31]
<i>Kinetic</i>		
Pseudo-first-order	$q_t = q_e (1 - e^{-k_1 t})$ (7)	[32]
Pseudo-second-order	$q_t = \frac{k_2 q_e^2 t}{1 + k_2 q_e t}$ (8)	[33]
Elovich	$q_t = \frac{1}{\beta} \ln(\alpha\beta) + \frac{1}{\beta} \ln t$ (9)	[34]

Table 2
Error functions used in nonlinear regression analyses

Error function	Mathematical expression	Reference
Sum of the squared errors (SSE)	$\sum_{i=1}^n (q_{e,calc} - q_{e,meas})_i^2$	[36]
Hybrid fractional error (HYBRID)	$\frac{100}{n-p} \sum_{i=1}^n \left[\frac{(q_{e,calc} - q_{e,meas})_i^2}{q_{e,meas}} \right]_i$	[36]
Average relative error (ARE)	$\frac{100}{n} \left \frac{q_{e,calc} - q_{e,meas}}{q_{e,meas}} \right _i$	[37]
Marquardt's percent standard deviation (MPSD)	$100 \sqrt{\frac{1}{n-p} \sum_{i=1}^n \left(\frac{q_{e,calc} - q_{e,meas}}{q_{e,meas}} \right)_i^2}$	[38]
Sum of the absolute errors (EABS)	$\sum_{i=1}^n q_{e,calc} - q_{e,meas} _i$	[36]

et al. [25], who performed the kinetic, equilibrium, and thermodynamic experiments to characterize the phosphate sorption onto iron oxide nanoparticles. Equilibrium batch experiments were conducted as a function of phosphate concentration. Six isotherm models (Table 1) were used to analyze the equilibrium data. Kinetic batch experiments were also performed as a function of shaking time. Three kinetic models (Table 1) were used to analyze the kinetic data through nonlinear regression. Various error functions (Table 2) were used to minimize the error distribution between experimental data and predicted model fits in the optimization process [35].

2. Materials and methods

2.1. Batch experiments

Phosphate removal by iron oxide nanoparticles was conducted under batch conditions. Iron oxide nanoparticles used in the experiments were synthesized by the co-precipitation method described in [25]. The characteristics of iron oxide nanoparticles were described elsewhere [25]. Briefly, synthesized iron oxides were nanosized particles composed of maghemite ($\gamma\text{-Fe}_2\text{O}_3$) and goethite ($\alpha\text{-FeOOH}$) with a BET specific area of $82.2\text{ m}^2/\text{g}$. For the batch experiments, the desired phosphate (P) solution was prepared by diluting the stock solution ($1,000\text{ mg/L}$), which was made from potassium dichromate (KH_2PO_4). All batch experiments were performed in triplicate using 50 mL polypropylene conical tubes. First, equilibrium batch experiments were conducted in a 30 mL solution (initial P concentration = $0.5\text{--}20\text{ mg/L}$; adsorbent doses = $0.1, 0.2, 0.3, 0.4, 0.5,$ and 0.6 g/L). The tubes were shaken at 30°C and 100 rpm using a shaking incubator (Daihan Science, Korea). The samples were collected after 24 h of shaking time and filtered through a $0.45\text{-}\mu\text{m}$ membrane filter. The phosphate was analyzed by the ascorbic acid method [39]. Phosphate concentrations were measured at a wavelength of 880

nm using a UV-vis spectrophotometer (Helios, Thermo Scientific, Waltham, MA, USA). Second, kinetic batch experiments were performed in a 30 mL solution (initial P concentration = $1, 2, 4, 6, 8,$ and 10 mg/L ; adsorbent dose = 0.6 g/L). The tubes were shaken at 30°C and 100 rpm using a shaking incubator,

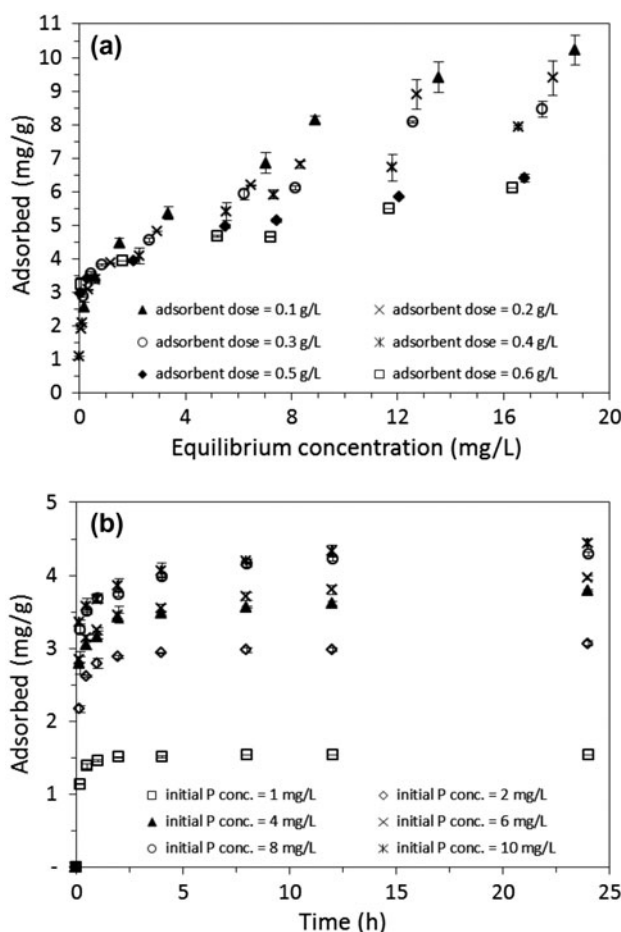


Fig. 1. Phosphate sorption experimental data: (a) equilibrium; (b) kinetic.

and the samples were collected after various shaking times from 10 min to 24 h.

2.2. Nonlinear regression with error functions

To determine the optimum isotherm and kinetic model parameters for the experimental data, various error functions were used in the error analysis (Table 2). Five different error functions were examined to determine parameters for each model by minimizing the respective errors using the solver add-in with Microsoft's spread sheet, Excel (Microsoft corporation, 1994). To compare the five error values, the results of each set were normalized and summed (SNE). SNE used to find the best error function for analyzing models and obtaining parameters. Coefficient of determination (R^2) and Chi-square (χ^2) analyses were used to evaluate the best fit of kinetic or equilibrium models with experimental data. The best fit model was selected by the highest R^2 and lowest χ^2 .

3. Results and discussion

3.1. Nonlinear regression with isotherm models

The equilibrium batch data for phosphate sorption onto iron oxide nanoparticles under various adsorbent doses (initial P concentration = 0.5–20 mg/L; adsorbent doses = 0.1, 0.2, 0.3, 0.4, 0.5, and 0.6 g/L; shaking time = 24 h) are presented in Fig. 1(a). At an adsorbent dose of 0.1 g/L, the sorption capacities were in the range of 2.57–10.22 mg/g. The sorption capacities at an adsorbent dose of 0.2 g/L varied from 1.90 to 9.39 mg/g, whereas the sorption capacities at 0.3 g/L were in the range of 2.88–8.45 mg/g. At an adsorbent dose of 0.4 g/L, the sorption capacities were in the range of 1.10–7.93 mg/g. The sorption capacities at an adsorbent dose of 0.5 g/L varied from 2.97 to 6.40 mg/g, whereas the sorption capacities at 0.6 g/L were in the range of 3.23–6.10 mg/g. The equilibrium data (Fig. 1(a)) were analyzed by two-parameter isotherms with five error functions.

Table 3
Error function values and model parameters of two-parameter isotherms (adsorbent dose = 0.6 g/L)

	SSE	HYBRID	ARE	MPSD	EABS
<i>Langmuir</i>					
Q_m (mg/g)	5.03	4.92	4.69	4.69	4.69
K_L (L/mg)	25.75	28.14	34.33	34.33	34.33
SSE	2.60	2.66	3.13	3.13	3.13
HYBRID	13.22	12.93	14.15	14.15	14.15
ARE	11.48	10.75	9.29	9.29	9.29
MPSD	34.44	32.26	27.86	27.86	27.86
EABS	3.32	3.19	2.93	2.93	2.93
SNE	4.76	4.60	4.50	4.50	4.50
<i>Freundlich</i>					
K_F (L/g)	4.00	4.04	4.06	4.06	3.63
$1/n$	0.12	0.11	0.08	0.08	0.17
SSE	0.71	0.74	1.30	1.30	1.18
HYBRID	3.88	3.74	5.65	5.64	8.36
ARE	7.14	6.91	5.94	5.95	7.64
MPSD	21.43	20.72	17.83	17.83	22.92
EABS	1.92	1.93	1.91	1.91	1.78
SNE	3.87	3.83	4.22	4.22	4.83
<i>Temkin</i>					
A_T (L/g)	9,751.00	19,429.11	294,084.9	294,269.2	294,300
b_T (J/mol)	5.54	5.95	7.69	7.69	7.69
SSE	1.02	1.05	1.59	1.59	1.59
HYBRID	5.34	5.18	6.93	6.93	6.93
ARE	8.37	7.92	6.54	6.54	6.54
MPSD	25.10	23.75	19.62	19.62	19.62
EABS	2.31	2.26	2.10	2.10	2.10
SNE	4.41	4.28	4.47	4.47	4.47

Note: Numbers in bold type represent the minimum values of relevant error function and SNE.

The estimated error function values and model parameters for an adsorbent dose of 0.6 g/L are provided in Table 3. In the Langmuir isotherm, the lowest SNE values were obtained from the error functions of average relative error (ARE) (4.50), Marquardt’s percent standard deviation (MPSD) (4.50), and sum of the absolute errors (EABS) (4.50). In the Freundlich and Temkin isotherms, the lowest SNE values were obtained from the HYBRID (Freundlich = 3.83; Temkin = 4.28). The equilibrium data (Fig. 1(a)) were also analyzed by three-parameter isotherms with five error functions. The estimated error function values and model parameters (adsorbent dose = 0.6 g/L) are provided in Table 4. In the Redlich–Peterson, Khan, and Sips isotherms, the lowest

SNE values were obtained from the HYBRID (Redlich–Peterson = 3.84; Khan = 3.84; Sips = 4.16).

The Freundlich isotherm fitted with five error functions for the equilibrium data (adsorbent dose = 0.6 g/L) are shown as an example in Fig. 2(a). The comparison of six isotherm models indicated that the Freundlich model had the lowest SNE value (3.83). The six isotherm models fitted with the HYBRID error function for the equilibrium data (adsorbent dose = 0.6 g/L) are also presented as an example in Fig. 2(b). The results also demonstrated that the HYBRID provided the best estimation of all isotherm models except the Langmuir model. Therefore, the HYBRID was selected to analyze the equilibrium data. In the literature, the HYBRID error function has been

Table 4
Error function values and model parameters of three-parameter isotherms (adsorbent dose = 0.6 g/L)

	SSE	HYBRID	ARE	MPSD	EABS
<i>Redlich–Peterson</i>					
K_R (L/g)	167,468.10	245,480.98	980,001	980,000	987,140.79
a_R (L/mg)	41,881.90	60,805.56	240,806.96	240,806.97	272,244.43
K_R/a_R (mg/g)	4.00	4.04	4.07	4.07	3.63
g	0.879	0.889	0.916	0.916	0.830
SSE	0.71	0.74	1.26	1.26	1.18
HYBRID	5.18	4.98	7.36	7.36	11.16
ARE	7.15	6.91	5.97	5.97	7.64
MPSD	24.76	23.94	20.69	20.69	26.47
EABS	1.92	1.93	1.92	1.92	1.78
SNE	3.89	3.84	4.22	4.22	4.86
<i>Khan</i>					
q_s (mg/g)	1.41	1.72	2.11	2.11	0.91
b_K	5,736.82	2,272.62	2,803.00	2,803.00	3,530.00
a_K	0.880	0.890	0.917	0.917	0.831
SSE	0.72	0.75	1.32	1.32	1.19
HYBRID	5.21	5.10	7.65	7.64	11.30
ARE	7.17	6.98	5.99	5.99	7.68
MPSD	24.84	24.17	20.75	20.75	26.61
EABS	1.93	1.95	1.93	1.93	1.79
SNE	3.86	3.84	4.23	4.23	4.82
<i>Sips</i>					
q_m (mg/g)	28.31	34.70	30.01	30.03	30.00
a_s	0.17	0.13	0.16	0.16	0.16
β_s	0.14	0.12	0.10	0.10	0.10
SSE	0.77	0.79	1.35	1.35	1.35
HYBRID	5.49	5.27	7.83	7.83	7.83
ARE	7.38	7.05	6.05	6.05	6.05
MPSD	25.58	24.43	20.97	20.97	20.97
EABS	2.00	1.98	1.95	1.95	1.95
SNE	4.27	4.16	4.61	4.61	4.61

Note: Numbers in bold type represent the minimum values of relevant error function and SNE.

selected by researchers to determine the optimized isotherm model parameter values. Allen et al. [40] reported that the sorption isotherms for two basic dyes (Basic Yellow 21 and Basic Red 22) onto an adsorbent (kudzu) are generally better represented by the HYBRID. Gunay [41] also used the HYBRID to obtain isotherm parameters for ammonium exchange by natural clinoptilolite because the HYBRID was shown to provide the lowest SNE values.

Nonlinear regression analyses of six isotherms for the equilibrium data are summarized in Table 5. The HYBRID error function, R^2 , and χ^2 along with optimized parameter values for the six isotherm models are shown in Table 5. At an adsorbent dose of 0.1 g/L, the Redlich–Peterson, Freundlich, Khan, and Sips models had the same highest R^2 (0.985) and the same

lowest χ^2 (0.129). Considering both R^2 and χ^2 , the fitting degree of isotherm models were classified as Freundlich = Redlich–Peterson = Khan = Sips > Temkin > Langmuir. At an adsorbent dose of 0.2 g/L, the Redlich–Peterson, Freundlich, Khan, and Sips models had the same highest R^2 (0.967), whereas the models showed slightly different χ^2 values. The Redlich–Peterson (Freundlich) model had the best model fit followed by Khan = Sips > Temkin > Langmuir. At an adsorbent dose of 0.3 g/L, the Redlich–Peterson, Freundlich, Khan, and Sips models had the same highest R^2 (0.943), whereas the models showed slightly different χ^2 values. The Redlich–Peterson (Freundlich) model had the best model fit followed by Sips > Khan > Temkin > Langmuir. At an adsorbent dose of 0.4 g/L, the Redlich–Peterson and Freundlich had the same highest R^2 (0.989) and the same lowest χ^2 (0.093). The Redlich–Peterson (Freundlich) model had the best model fit followed by Khan > Sips > Temkin > Langmuir. At 0.5 g/L, the Redlich–Peterson (Freundlich) model had the highest R^2 (0.899) and lowest χ^2 (0.234). Thus, the fitting degree of isotherm models were classified as Redlich–Peterson (Freundlich) > Sips > Khan > Temkin > Langmuir. The same trend could be found at 0.6 g/L, showing that the Freundlich and Redlich–Peterson models had the same R^2 (0.855) and χ^2 (0.149) values. Considering both χ^2 and R^2 , the Redlich–Peterson (Freundlich) model was selected as the best-fitting model for the equilibrium data. Note that the Freundlich isotherm is one of special case of the Redlich–Peterson isotherm [10]. The Redlich–Peterson isotherm fitted with the HYBRID error function for the equilibrium data is shown in Fig. 3. The optimum parameter values of $K_R/a_R = 3.59\text{--}4.15$ mg/g and $g = 0.69\text{--}0.89$ were determined from the Redlich–Peterson model (Table 5).

In our study, the Redlich–Peterson (Freundlich) isotherm was the best model for the equilibrium data. Ayoob and Gupta [42] performed isotherm studies to examine the adsorptive removal of fluoride by alumina cement granules. Three isotherms (Freundlich, Langmuir, and Dubinin–Radushkevich) were used to analyze the equilibrium data using five error functions. From the χ^2 analysis with minimum SNE values, the Freundlich was determined to be the best-fit isotherm for the data. Ho et al. [10] performed regression analysis for the sorption isotherm data of basic dyes onto sugarcane dust. Among the three (Freundlich, Langmuir, and Redlich–Peterson) isotherms, the Redlich–Peterson was determined to be the best-fitting isotherm for the equilibrium data from the χ^2 analysis. Other researchers reported that isotherms such as Langmuir and Sips models provided the best fit for their experimental data. Kumar et al. [18] performed

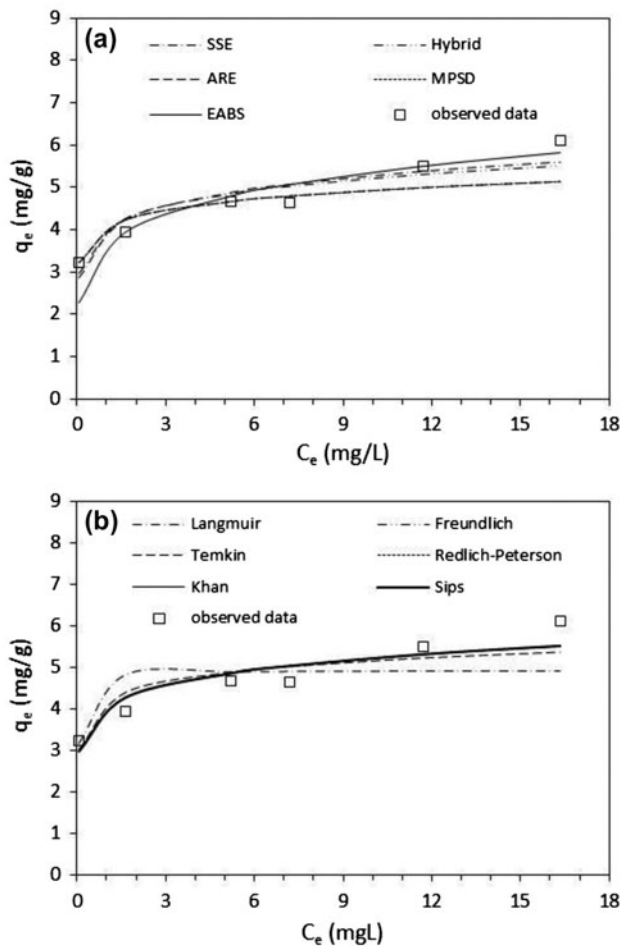


Fig. 2. Nonlinear regression analyses for equilibrium data (adsorbent dose = 0.6 g/L): (a) comparison of Freundlich isotherm model fits among five error functions; (b) comparison of model fits from HYBRID error function among six isotherms. Error function values and model parameters are provided in Tables 3 and 4.

Table 5
Nonlinear regression analyses of two- and three-parameter isotherms for equilibrium data at various adsorbent dosages

	0.1 g/L	0.2 g/L	0.3 g/L	0.4 g/L	0.5 g/L	0.6 g/L
<i>Langmuir</i>						
Q_m (mg/g)	8.95	7.62	6.70	6.27	4.80	4.92
K_L (L/mg)	0.91	1.43	2.63	2.45	87.75	28.14
HYBRID	42.78	61.84	43.28	56.89	31.42	13.22
R^2	0.850	0.784	0.688	0.874	0.368	0.485
χ^2	1.711	2.474	1.731	1.996	1.257	0.517
<i>Freundlich</i>						
K_F (L/g)	3.98	3.89	4.07	3.58	4.15	4.04
$1/n$	0.31	0.29	0.23	0.26	0.12	0.11
HYBRID	3.22	6.31	6.84	2.32	5.87	3.74
R^2	0.985	0.967	0.943	0.989	0.889	0.855
χ^2	0.129	0.252	0.274	0.093	0.234	0.149
<i>Temkin</i>						
A_T (L/g)	21.22	63.89	78.35	289.05	26,897.32	294,300
b_T (J/mol)	1.70	2.30	2.49	3.36	5.92	7.69
HYBRID	19.48	27.50	15.84	20.21	9.68	6.93
R^2	0.899	0.820	0.848	0.890	0.790	0.782
χ^2	0.779	1.100	0.634	0.808	0.387	0.207
<i>Redlich–Peterson</i>						
K_R (L/g)	244,550.00	243,724.00	245,734.92	91,305.62	245,963.07	245,480.98
a_R (L/mg)	61,504.37	63,025.7	60,372.61	25,447.89	59,173.77	60,805.56
K_R/a_R (mg/g)	3.98	3.87	4.07	3.59	4.15	4.04
g	0.69	0.71	0.77	0.74	0.88	0.89
HYBRID	4.29	8.42	9.13	3.09	7.84	4.98
R^2	0.985	0.967	0.943	0.989	0.889	0.855
χ^2	0.129	0.252	0.274	0.093	0.234	0.149
<i>Khan</i>						
q_s (mg/g)	0.26	0.31	0.67	0.45	1.70	1.72
b_K	5,851.30	6,159.72	2,272.62	3,178.95	2,272.62	2,272.62
a_K	0.685	0.71	0.767	0.743	0.884	0.890
HYBRID	4.30	8.44	9.17	3.12	8.38	5.10
R^2	0.985	0.967	0.943	0.986	0.884	0.853
χ^2	0.129	0.253	0.275	0.094	0.251	0.152
<i>Sips</i>						
q_m (mg/g)	2,235.84	3,885.47	2,080.36	2,450.93	1,128.64	34.70
a_s	0.002	0.001	0.002	0.001	0.004	0.13
$1/n$	0.32	0.29	0.23	0.26	0.12	0.12
HYBRID	4.31	8.44	9.15	3.10	7.84	5.27
R^2	0.985	0.967	0.943	0.986	0.889	0.842
χ^2	0.129	0.253	0.275	0.093	0.235	0.158

Note: Numbers in bold type represent the minimum values of R^2 and χ^2 .

isotherm and thermodynamic studies for the adsorption of methylene blue onto activated carbon. They determined the optimum isotherm from three (Freundlich, Langmuir, and Redlich–Peterson) isotherms by nonlinear regression using six error functions. Both Langmuir and Redlich–Peterson were shown to be the

optimum isotherms for methylene blue adsorption onto activated carbon. MPD provides the best parameters for the Langmuir isotherm, whereas the coefficient of determination is the best for the Redlich–Peterson isotherm. Ho et al. [35] analyzed the experimental data for the sorption of divalent ions (Cu, Ni,

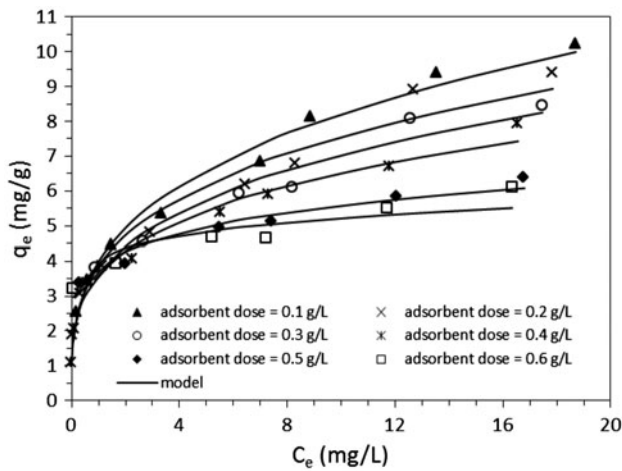


Fig. 3. Nonlinear regression analyses for equilibrium data at six different adsorbent doses with Redlich–Peterson isotherm using HYBRID error function. Error function values and model parameters are provided in Table 5.

and Pb) onto peat with six (Freundlich, Langmuir, Redlich–Peterson, Toth, Temkin, Dubinin–Radushkevich, and Sips) isotherms with error functions. They reported that Sips model generally provided the best fit for the experimental data. Ng et al. [43] performed nonlinear regression analysis using five error functions to determine the optimum isotherm for the equilibrium sorption of lead ions onto chitosan among three (Freundlich, Langmuir, and Redlich–Peterson) isotherms. They reported that both Langmuir and Redlich–Peterson are the optimum isotherms for lead sorption ions onto chitosan, and the SSE error function provides the best parameters for the isotherms.

3.2. Nonlinear regression with kinetic models

The kinetic data for phosphate sorption onto iron oxide nanoparticles under various initial P concentrations (initial P concentration = 1, 2, 4, 6, 8, and 10 mg/L; adsor-

Table 6
Error function values and model parameters of kinetic sorption models (initial P concentration = 2 mg/L)

	SSE	HYBRID	ARE	MPSD	EABS
<i>Pseudo-first-order</i>					
q_e (mg/g)	2.91	2.90	2.94	2.94	2.94
k_1 (1/h)	7.77	7.89	8.03	8.03	8.03
SSE	0.11	0.11	0.12	0.12	0.12
HYBRID	0.65	0.65	0.71	0.71	0.71
ARE	4.55	4.51	4.07	4.07	4.07
MPSD	11.14	11.04	9.97	9.97	9.97
EABS	0.76	0.75	0.68	0.68	0.68
SNE	4.83	4.80	4.68	4.68	4.68
<i>Pseudo-second-order</i>					
q_e (mg/g)	3.00	3.00	2.98	2.98	2.98
k_2 (g/mg/h)	4.95	5.00	5.34	5.34	5.34
SSE	0.01	0.01	0.01	0.01	0.01
HYBRID	0.05	0.05	0.06	0.06	0.06
ARE	1.19	1.15	1.04	1.04	1.04
MPSD	2.91	2.82	2.55	2.55	2.55
EABS	0.20	0.19	0.18	0.18	0.18
SNE	4.83	4.72	4.65	4.65	4.65
<i>Elovich</i>					
α (mg/g/h)	2.67×10^6	1.22×10^6	2.60×10^6	2.60×10^6	2.60×10^6
β (g/mg)	6.26	5.98	6.28	6.28	6.28
SSE	0.10	0.10	0.10	0.10	0.10
HYBRID	0.64	0.63	0.64	0.64	0.64
ARE	4.81	4.97	4.80	4.80	4.80
MPSD	11.79	12.17	11.75	11.75	11.76
EABS	0.76	0.80	0.76	0.76	0.76
SNE	4.88	4.99	4.87	4.88	4.87

Note: Numbers in bold type represent the minimum values of relevant error function and SNE.

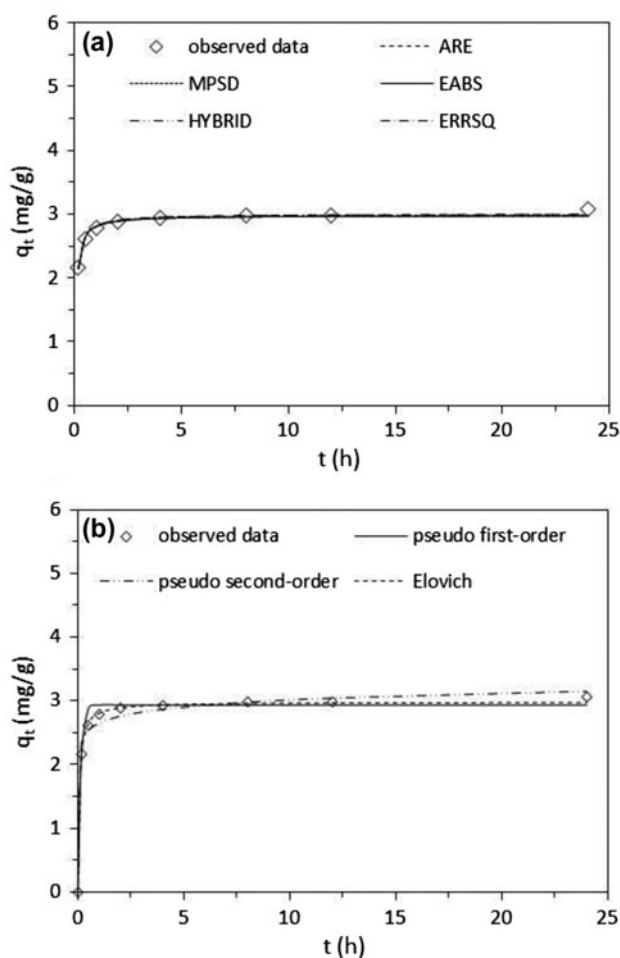


Fig. 4. Nonlinear regression analyses for kinetic data (initial P concentration = 2 mg/L): (a) comparison of pseudo-second-order model fits among five error functions; (b) comparison of model fits from EABS error function among three kinetic models. Error function values and model parameters are provided in Tables 6 and 7.

bent dose = 0.6 g/L; and shaking time = 10 min–24 h) are presented in Fig. 1(b). As the initial phosphate concentration increased, the phosphate sorption capacity increased at the same reaction time. The kinetic data (Fig. 1(b)) were analyzed by three kinetic models with five error functions. The estimated error function values and model parameters for an initial P concentration of 2 mg/L are provided in Table 6. In the pseudo-first-order and pseudo-second-order models, the lowest SNE values were obtained from the error functions of the ARE, MPSD, and EABS (pseudo-first-order = 4.68 and pseudo-second-order = 4.65). In the Elovich model, the lowest SNE values were obtained from the ARE (4.87) and EABS (4.87) error functions. The pseudo-second-order model fitted with five error functions for the kinetic data (initial

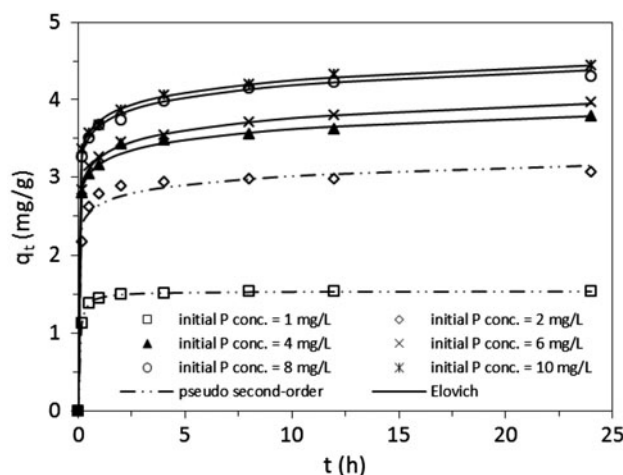


Fig. 5. Nonlinear regression analyses for kinetic data at six different P concentrations with pseudo-second-order or Elovich models using EABS error function. Error function values and model parameters are provided in Table 7.

P concentration = 2 mg/L) is shown as an example in Fig. 4(a). Comparison of the three kinetic models indicated that the pseudo-second-order model had the lowest SNE value (4.65). Also, both the ARE and EABS provided the best estimation of all kinetic models. In this study, the EABS was selected to analyze the kinetic data. Three kinetic models fitted with the EABS error function for the kinetic data (initial P concentration = 2 mg/L) are presented in Fig. 4(b).

The nonlinear regression analyses of three kinetic models are presented in Fig. 5. The EABS, R^2 , and χ^2 along with optimized parameter values for the kinetic models are provided in Table 7. At an initial P concentration of 1 mg/L, the pseudo-second-order model had the highest R^2 (0.998) and lowest χ^2 (0.001). In the case of χ^2 , the pseudo-second-order model was also the best-fitting model followed by the pseudo-first-order then Elovich models. Considering both R^2 and χ^2 , the pseudo-second-order model was the best-fitting model followed by the pseudo-first-order then Elovich models. At an initial P concentration of 2 mg/L, the pseudo-second-order model had the highest R^2 (0.980) and lowest χ^2 (0.004). In the case of χ^2 , the pseudo-second-order model was also the best-fitting model followed by the Elovich and then pseudo-first-order models. The pseudo-second-order model was the best-fitting model followed by the pseudo-first-order then Elovich models. At 4 mg L⁻¹, the Elovich model had the highest R^2 (0.976) and lowest χ^2 (0.006). Thus, the fitting degree of the kinetic models was classified as Elovich > pseudo-second-order > pseudo-first-order.

Table 7

Nonlinear regression analyses of kinetic sorption models for kinetic data at various initial P concentrations

	1 mg/L	2 mg/L	4 mg/L	6 mg/L	8 mg/L	10 mg/L
<i>Pseudo-first-order</i>						
q_e (mg/g)	1.51	2.94	3.48	3.54	3.98	4.06
k_1 (1/h)	8.36	8.03	9.77	9.70	10.24	10.59
EABS	0.23	0.68	1.31	1.59	1.73	1.85
R^2	0.896	0.878	0.511	0.461	0.460	0.397
χ^2	0.010	0.042	0.120	0.142	0.143	0.166
<i>Pseudo-second-order</i>						
q_e (mg/g)	1.54	2.98	3.52	3.59	4.02	4.09
k_2 (g/mg/h)	10.83	5.34	5.59	6.06	6.22	6.74
EABS	0.04	0.18	0.90	1.15	1.28	1.41
R^2	0.998	0.980	0.772	0.647	0.622	0.538
χ^2	0.001	0.004	0.047	0.074	0.071	0.091
<i>Elovich</i>						
α (mg/g/h)	4.80×10^6	2.60×10^6	2.30×10^6	6.58×10^5	2.50×10^6	3.60×10^5
β (g/mg)	13.07	6.28	5.14	4.58	4.43	4.45
EABS	0.47	0.76	0.26	0.15	0.21	0.18
R^2	0.762	0.839	0.976	0.995	0.986	0.993
χ^2	0.027	0.038	0.006	0.002	0.004	0.002

Note: Numbers in bold type represent the minimum values of R^2 and χ^2 .

The same trend was found at 6, 8, and 10 mg/L, showing that the fitting degree of the kinetic models could be classified as Elovich > pseudo-second-order > pseudo-first-order. The Elovich model had the highest R^2 and lowest χ^2 . The Elovich (or pseudo-second-order) model was selected as the best model for the kinetic data. From the Elovich model, the optimum parameter values of $\alpha = (3.60 \times 10^5) - (4.80 \times 10^6)$ mg/g/h and $\beta = 4.43 - 13.07$ g/mg were determined (Table 7). The Elovich model has been used in several studies to describe the sorption of phosphate onto adsorbents [44,45]. Ruan and Gilkes [46] showed that phosphate sorption kinetics onto synthetic iron oxides such as goethite and hematite can be well described by the Elovich equation. Wang et al. [47] also reported that the adsorption kinetics of phosphate onto lead-zinc tailings can be best described by the Elovich equation.

4. Conclusions

The best kinetic and isotherm models for phosphate sorption onto iron oxide nanoparticles were determined through nonlinear regression analysis. Equilibrium model analyses showed that the Redlich-Peterson (Freundlich) model was found to provide the best fit to the experimental data in the equilibrium model analyses, and the optimum parameter values were obtained by the HYBRID error function. Kinetic

model analyses demonstrated that the Elovich (or pseudo-second-order) model was found to provide the best fit to the kinetic data in the kinetic model analyses, and the optimum parameter values produced by the EABS error function.

Acknowledgments

This work was supported by the Korea Institute of Science and Technology (KIST) Institutional Program (Project No. 2E24563).

Nomenclature

a_K	— Khan isotherm model exponent
a_R	— Redlich-Peterson isotherm constant (L/mg)
a_S	— Sips isotherm model constant (L/mg)
A_T	— Temkin isotherm constant (L/g)
B	— Langmuir isotherm constant (L/mg)
b_K	— Khan isotherm model constant (L/mg)
b_T	— Temkin isotherm constant
C_e	— equilibrium concentration (mg/L)
C_0	— adsorbate initial concentration (mg/L)
C_s	— adsorbate monolayer saturation concentration (mg/L)
g	— Redlich-Peterson isotherm exponent
k_1	— rate constant of adsorption (/h)

k_2	— rate constant of pseudo-second-order adsorption (mg/g/h)
K_F	— Freundlich isotherm constant (L/g)
K_L	— Langmuir isotherm constant (L/mg)
K_R	— Redlich–Peterson isotherm constant (L/g)
K_S	— Sips isotherm model constant (L/g)
n	— number of data points
$1/n$	— Freundlich isotherm constant
p	— number of isotherm parameters
q_e	— amount of phosphate adsorbed on the adsorbent at equilibrium (mg/g)
$q_{e,calc}$	— calculated phosphate adsorption capacity at equilibrium (mg/g)
$q_{e,meas}$	— measured phosphate adsorption capacity at equilibrium (mg/g)
$\bar{q}_{e,meas}$	— average of measured phosphate adsorption capacity at equilibrium (mg/g)
q_s	— theoretical isotherm saturation capacity (mg/g)
q_t	— amount of phosphate adsorbed on the adsorbent at time t (mg/g)
$q_{t,calc}$	— calculated phosphate adsorption capacity at time t (mg/g)
$\bar{q}_{t,meas}$	— average of measured phosphate adsorption capacity at time t (mg/g)
R	— universal gas constant (8.314 J/mol K)
R^2	— coefficient of determination
T	— temperature (K)
α	— initial adsorption rate (mg/g/h)
β	— adsorption constant (g/mg)
β_s	— Sips isotherm model exponent

References

- [1] N. Gangoli, G. Thodos, Phosphate adsorption studies, *J. Water Pollut. Cont. Fed.* 45 (1973) 842–849.
- [2] A. Dąbrowski, Adsorption—from theory to practice, *Adv. Coll. Interface Sci.* 93 (2001) 135–224.
- [3] K.Y. Foo, B.H. Hameed, Insights into the modeling of adsorption isotherm systems, *Chem. Eng. J.* 156 (2010) 2–10.
- [4] S. Sen Gupta, K.G. Bhattacharyya, Kinetics of adsorption of metal ions on inorganic materials: A review, *Adv. Coll. Interface Sci.* 162 (2011) 39–58.
- [5] L. Zhang, S. Hong, J. He, F. Gan, Y.S. Ho, Adsorption characteristic studies of phosphorus onto laterite, *Desalin. Water Treat.* 25 (2011) 98–105.
- [6] D. Karadag, Y. Koc, M. Turan, M. Ozturk, A comparative study of linear and non-linear regression analysis for ammonium exchange by clinoptilolite zeolite, *J. Hazard. Mater.* 144 (2007) 432–437.
- [7] Y.S. Ho, Selection of optimum sorption isotherm, *Carbon* 42 (2004) 2113–2130.
- [8] Y.S. Ho, Isotherms for the sorption of lead onto peat: Comparison of linear and non-linear methods, *Polish J. Environ. Stud.* 15 (2006) 81–86.
- [9] Y.S. Ho, Second-order kinetic model for the sorption of cadmium onto tree fern: A comparison of linear and non-linear methods, *Water Res.* 40 (2006) 119–125.
- [10] Y.S. Ho, W.T. Chiu, C.C. Wang, Regression analysis for the sorption isotherms of basic dyes on sugarcane dust, *Bioresour. Technol.* 96 (2005) 1285–1291.
- [11] Y.S. Ho, A.E. Ofomaja, Kinetics and thermodynamics of lead ion sorption on palm kernel fibre from aqueous solution, *Proc. Biochem.* 40 (2005) 3455–3461.
- [12] Y.S. Ho, A.E. Ofomaja, Pseudo-second-order model for lead ion sorption from aqueous solutions onto palm kernel fiber, *J. Hazard. Mater.* 129 (2006) 137–142.
- [13] K.V. Kumar, S. Sivanesan, Comparison of linear and non-linear method in estimating the sorption isotherm parameters for safranin onto activated carbon, *J. Hazard. Mater.* 123 (2005) 288–292.
- [14] K.V. Kumar, S. Sivanesan, Isotherm parameters for basic dyes onto activated carbon: Comparison of linear and non-linear method, *J. Hazard. Mater.* 129 (2006) 147–150.
- [15] K.V. Kumar, Comparative analysis of linear and non-linear method of estimating the sorption isotherm parameters for malachite green onto activated carbon, *J. Hazard. Mater.* 136 (2006) 197–202.
- [16] K.V. Kumar, S. Sivanesan, Pseudo second order kinetics and pseudo isotherms for malachite green onto activated carbon: Comparison of linear and non-linear regression methods, *J. Hazard. Mater.* 136 (2006) 721–726.
- [17] K.V. Kumar, K. Porkodi, F. Rocha, Comparison of various error functions in predicting the optimum isotherm by linear and non-linear regression analysis for the sorption of basic red 9 by activated carbon, *J. Hazard. Mater.* 150 (2008) 158–165.
- [18] K.V. Kumar, K. Porkodi, F. Rocha, Isotherms and thermodynamics by linear and non-linear regression analysis for the sorption of methylene blue onto activated carbon: Comparison of various error functions, *J. Hazard. Mater.* 151 (2008) 794–804.
- [19] D.G. Kinniburgh, General purpose adsorption isotherms, *Environ. Sci. Technol.* 20(9) (1986) 895–904.
- [20] D.J. Conley, H.W. Paerl, R.W. Howarth, D.F. Boesch, S.P. Seitzinger, K.E. Havens, C. Lancelot, G.E. Likens, Ecology: Controlling eutrophication: Nitrogen and phosphorus, *Science* 323 (2009) 1014–1015.
- [21] K.C. Ruttenger, D.J. Sulak, Sorption and desorption of dissolved organic phosphorus onto iron (oxyhydr) oxides in seawater, *Geochim. Cosmochim. Acta* 75 (2011) 4095–4112.
- [22] C. Luengo, M. Brigante, J. Antelo, M. Avena, Kinetics of phosphate adsorption on goethite: Comparing batch adsorption and ATR-IR measurements, *J. Colloid Interface Sci.* 300 (2006) 511–518.

- [23] I. de Vicente, A. Merino-Martos, L. Cruz-Pizarro, J. de Vicente, On the use of magnetic nano and microparticles for lake restoration, *J. Hazard. Mater.* 181 (2010) 375–381.
- [24] L. Zeng, X. Li, J. Liu, Adsorptive removal of phosphate from aqueous solutions using iron oxide tailings, *Water Res.* 38 (2004) 1318–1326.
- [25] S.Y. Yoon, C.G. Lee, J.A. Park, J.H. Kim, S.B. Kim, S.H. Lee, J.W. Choi, Kinetic, equilibrium and thermodynamic studies for phosphate adsorption to magnetic iron oxide nanoparticles, *Chem. Eng. J.* 236 (2014) 341–347.
- [26] I. Langmuir, The constitution and fundamental properties of solids and liquids. Part I. Solids, *J. Am. Chem. Soc.* 38 (1916) 2221–2295.
- [27] H.M.F. Freundlich, Over the adsorption in solution, *J. Phys. Chem.* 57 (1906) 385–471.
- [28] M.I. Tempkin, V. Pyzhev, Kinetics of ammonia synthesis on promoted iron catalyst, *Acta Phys. Chim. USSR* 12 (1940) 327–356.
- [29] O. Redlich, D.L. Peterson, A useful adsorption isotherm, *J. Phys. Chem.* 63 (1959) 1024–1026.
- [30] A.R. Khan, R. Atallah, A. Al-Haddad, Equilibrium adsorption studies of some aromatic pollutants from dilute aqueous solutions on activated carbon at different temperatures, *J. Colloid Interface Sci.* 194 (1997) 154–165.
- [31] R. Sips, Combined form of Langmuir and Freundlich equations, *J. Chem. Phys.* 16 (1948) 490–495.
- [32] S. Lagergren, About the theory of so-called adsorption of soluble substances, *Kung. Sven. Vetén. Hand.* 24 (1898) 1–39.
- [33] Y.S. Ho, G. McKay, A comparison of chemisorption kinetic models applied to pollutant removal on various sorbents, *Proc. Safe. Environ. Protect.* 76 (1998) 332–340.
- [34] J. Zeldowitsch, About the mechanism of the catalytic oxidation of CO on MnO₂, *Acta Physicochim. URSS* 1 (1934) 364–449.
- [35] Y.S. Ho, J.F. Porter, G. McKay, Equilibrium isotherm studies for the sorption of divalent metal ions onto peat: Copper, nickel and lead single component systems, *Water Air Soil Pollut.* 141 (2002) 1–33.
- [36] J.F. Porter, G. McKay, K.H. Choy, The prediction of sorption from a binary mixture of acidic dyes using single- and mixed-isotherm variants of the ideal adsorbed solute theory, *Chem. Eng. Sci.* 54 (1999) 5863–5885.
- [37] A. Kapoor, R.T. Yang, Correlation of equilibrium adsorption data of condensable vapours on porous adsorbents. *Gas Sep. Purif.* 3 (1989) 187–192.
- [38] D.W. Marquardt, An algorithm for least-squares estimation of nonlinear parameters, *J. Soc. Ind. Appl. Math.* 11 (1963) 431–441.
- [39] APHA, Standard Methods for the Examination of Water and Wastewater, American Public Health Association, Washington, DC, 1995.
- [40] S.J. Allen, Q. Gan, R. Matthews, P.A. Johnson, Comparison of optimised isotherm models for basic dye adsorption by kudzu, *Bioresour. Technol.* 88 (2003) 143–152.
- [41] A. Gunay, Application of nonlinear regression analysis for ammonium exchange by natural (Bigadiç) clinoptilolite, *J. Hazard. Mater.* 148 (2007) 708–713.
- [42] S. Ayoob, A.K. Gupta, Insights into isotherm making in the sorptive removal of fluoride from drinking water, *J. Hazard. Mater.* 152 (2008) 976–985.
- [43] J.C.Y. Ng, W.H. Cheung, G. McKay, Equilibrium studies for the sorption of lead from effluents using chitosan, *Chemosphere* 52 (2003) 1021–1030.
- [44] S.H. Chien, W.R. Clayton, Application of elovich equation to the kinetics of phosphate release and sorption in soils, *Soil Sci. Soc. Am. J.* 44 (1980) 265–268.
- [45] H. Kiose, Application of S-shaped Z(t) plots to the kinetics of phosphate sorption by a soil of different phosphorus status, *Geoderma* 61 (1994) 61–70.
- [46] H.D. Ruan, R.J. Gilkes, Kinetics of phosphate sorption and desorption by synthetic aluminous goethite before and after thermal transformation to hematite, *Clay Miner.* 31 (1996) 63–74.
- [47] S. Wang, R. Yuan, X. Yu, C. Mao, Adsorptive removal of phosphate from aqueous solutions using lead-zinc tailings, *Water Sci. Technol.* 67 (2013) 983–988.